International Journal of Bifurcation and Chaos

The structure and evolution of confined tori near a Hamiltonian Hopf Bifurcation

M. KATSANIKAS
Research Center for Astronomy, Academy of Athens
Soranou Efessiou 4, GR-11527 Athens, Greece

Section of Astrophysics, Astronomy and Mechanics,
Department of Physics, University of Athens, Greece
mkatsan@academyofathens.gr

P.A. PATSIS and G. CONTOPOULOS
Research Center for Astronomy, Academy of Athens
Soranou Efessiou 4, GR-11527 Athens, Greece
patsis@academyofathens.gr, gcontop@academyofathens.gr

Received (to be inserted by publisher)

We study the orbital behavior at the neighborhood of complex unstable periodic orbits in a 3D autonomous Hamiltonian system of galactic type. At a transition of a family of periodic orbits from stability to complex instability (also known as Hamiltonian Hopf Bifurcation) the four eigenvalues of the stable periodic orbits move out of the unit circle. Then the periodic orbits become complex unstable. In this paper we first integrate initial conditions close to the ones of a complex unstable periodic orbit, which is close to the transition point. Then, we plot the consequents of the corresponding orbit in a 4D surface of section. To visualize this surface of section we use the method of color and rotation [Patsis and Zachilas 1994]. We find that the consequents are contained in 2D "confined tori". Then, we investigate the structure of the phase space in the neighborhood of complex unstable periodic orbits, which are further away from the transition point. In these cases we observe clouds of points in the 4D surfaces of section. The transition between the two types of orbital behavior is abrupt.

Keywords: Chaos and Dynamical Systems, 4D surfaces of section, Hopf Bifurcation, Galactic Dynamics

1. Introduction

The aim of this paper is to study the orbital behavior at the neighborhood of a complex unstable periodic orbit in a 3D autonomous Hamiltonian system of galactic type. Complex instability is a type of instability of periodic orbits that appears in Hamiltonian systems of three or more degrees of freedom.

In order to study the dynamical behavior at the neighborhood of a complex unstable periodic orbit we use the method of surfaces of section [Poincaré 1892], which has many applications to Dynamical Astronomy [for a review see e.g. Contopoulos 2002]. A basic problem in Hamiltonian systems of three degrees of freedom is the visualization of the 4D surfaces of section. Let us assume the phase space of an autonomous Hamiltonian system, that has 6 dimensions, e.g. in Cartesian coordinates, $(x, y, z, \dot{x}, \dot{y}, \dot{z})$. For a given Jacobi constant a trajectory lies on a 5D manifold. In this manifold the surface of section is 4D. This does not allow us to visualize directly the surface of section.

Patsis and Zachilas [1994] proposed a method to visualize 4D spaces of section. It is based on rotation of the 3D projections of the figures in order to understand the geometry of the formed structures and on color for understanding the distribution of the consequents in the 4th dimension. We use for this application the "Mathematica" package [Wolfram 1999]. We work in Cartesian coordinates and we consider the $y = 0$ with $\dot{y} > 0$ cross section. A set of three coordinates (e.g. $(x, \dot{x}, \dot{z})$) are used for the 3D projection, while the fourth coordinate (in our example z) will determine the color of the consequents. There is a normalization of the color values in the [min(z), max(z)] interval, which is mapped to [0,1]. Following the intrinsic "Mathematica" subroutines our viewpoint is given in spherical coordinates. The unit for the distance d of the consequents of the surface of section from the observer is given by "Mathematica" in a special scaled coordinate system, in which the longest side of the bounding box has length 1. For all figures we use $d = 1$. The method associates the smooth distribution or the mixing of colors, with specific types of dynamical behavior in the 4th dimension [Patsis and Zachilas 1994][see also Katsanikas and Patsis 2011].

The calculation of the linear stability of a periodic orbit follows the method of Broucke [1969] and Hadjidemetriou [1975]. We first consider small deviations from its initial conditions and then integrate the orbit again to the next upward intersection. In this way a 4D map (Poincaré map) is established and relates the initial with the final point. The relation of the final deviations of this neighboring orbit from the periodic one, with the initially introduced deviations, can be written in vector form as $\xi = \mathrm{M}\ \xi_0$. Here ξ is the final deviation, ξ_0 is the initial deviation, and M is a 4×4 matrix, called the monodromy matrix. It can be shown, that the characteristic equation can be written in the form $\lambda^4 + a\lambda^3 + \beta\lambda^2 + a\lambda + 1 = 0$. Its solutions $\lambda_i,\ i = 1, 2, 3, 4$, due to the symplectic identity of the monodromy matrix, that obey the relations $\lambda_1\lambda_3 = 1$ and $\lambda_2\lambda_4 = 1$ can be written as:

$$\lambda_i, \frac{1}{\lambda_i} = \frac{-b_i \pm \sqrt{b_i^2 - 4}}{2}, i = 1, 2 \tag{1}$$

where

$$b_{1,2} = \frac{a \pm \sqrt{\Delta}}{2} \tag{2}$$

and

$$\Delta = a^2 - 4(\beta - 2) \tag{3}$$

The quantities b_1 and b_2 are called the stability indices. Following the notation of Contopoulos and Magnenat [1985], if $\Delta > 0$, $|b_1| < 2$ and $|b_2| < 2$, all four eigenvalues are complex on the unit circle and the periodic orbit is called "stable" (S). If $\Delta > 0$ and $|b_1| > 2$, $|b_2| < 2$ or $|b_1| < 2$, $|b_2| > 2$, the periodic orbit is called "simple unstable" (U). In this case two eigenvalues are on the real axis and two are complex on the unit circle. If $\Delta > 0$ and $|b_1| > 2$ and $|b_2| > 2$, the periodic orbit is called "double unstable" (DU) and the four eigenvalues are on the real axis. Finally, if $\Delta < 0$ the periodic orbit is called "complex unstable" (Δ). In this case the four eigenvalues are complex numbers and they are off the unit circle. For the generalization of this kind of instability in Hamiltonian systems of N degrees of freedom the reader may refer to Skokos [2001]. If we have a stable one-parameter (in our system the Jacobi constant) family of periodic orbits, the four eigenvalues of a stable periodic orbit are complex on the unit circle. By varying the parameter we have a pairwise collision of eigenvalues on two conjugate points of the unit circle. From the Krein-Moser theorem [e.g. Contopoulos 2002 p.298] we can decide if after the collision of the eigenvalues they will remain on the unit circle and the periodic orbits

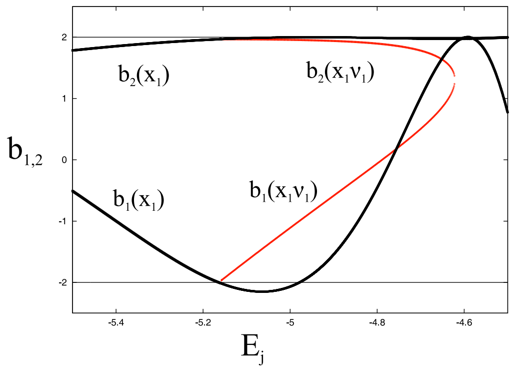

Fig. 1. Stability diagram for $-5.5 < E_j < -4.5$, that shows the stability of family x1 (with black line) and its bifurcating family of p.o. x1v1 (with red line).

of the family will stay stable, or if the eigenvalues will move out from the unit circle into the complex plane forming a complex quadruplet. In this latter case the periodic orbits of the family will become complex unstable and we will have a transition from stability to complex instability (also known as Hamiltonian Hopf Bifurcation). From an analytical point of view, the transition to complex instability has been studied using the Hamiltonian itself [Heggie 1985, Broer et al. 2007, Ollé et al. 2008] or 4D symplectic maps [Bridges et al. 1995]. In both cases, the approach consists of normal forms techniques [Ollé et al. 2005a,b] to simplify the Hamiltonian (or the map) and describe the local phase space structure near the critical periodic orbit (or fixed point in the discrete context). Such analysis shows, that the transition to complex instability gives rise to bifurcating invariant 2D tori in the flow context or invariant curves in 4D symplectic maps (as Poincaré map). The numerical computation of these invariant objects has been done for Hamiltonian systems of three degrees of freedom [Pfenniger 1985b, Ollé and Pfenniger 1998, Ollé et al. 2004] and for 4D symplectic maps [Pfenniger 1985a, Jorba and Ollé 2004]. It is remarkable, that there exists not one but two kinds of Hamiltonian Hopf bifurcations (as it happens in the usual dissipative setting), depending on the coefficients of the normal form [Van der Meer 1985]. These two kinds of bifurcations are usually called direct (supercritical) and inverse (subcritical). From a numerical point of view we can distinguish the two kinds of Hamiltonian Hopf bifurcation if we take firstly initial conditions in the vicinity of a complex unstable periodic orbit near the transition point from stability to complex instability. After that, we plot the consequents of the corresponding orbit in the surface of section. If the consequents are confined, we have a direct Hamiltonian Hopf Bifurcation. Otherwise, if the orbit escapes we have an inverse Hamiltonian Hopf Bifurcation. In this paper we examine the structure of the invariant surfaces in the 4D surface of section in the neighborhood of a complex unstable periodic orbit after a direct Hamiltonian Hopf bifurcation. The inverse Hopf bifurcation is not considered in the present paper, because in such a case all orbits close to a complex unstable periodic orbit escape [Jorba and Ollé 2004] and no confined structures appear.

2. The Hamiltonian System

The system we use for our applications is described in details in Katsanikas and Patsis [2011]. It rotates around its z-axis with angular velocity $\Omega_b = 60\ km\ s^{-1}\ kpc^{-1}$. The Hamiltonian of our system is:

$$H(x,y,z,\dot{x},\dot{y},\dot{z}) = \frac{1}{2}(\dot{x}^2+\dot{y}^2+\dot{z}^2)+\Phi(x,y,z) - \frac{1}{2}\Omega_b^2(x^2+y^2), \qquad (4)$$

where $\Phi(x,y,z)$ is our potential. The potential $\Phi(x,y,z)$ in its axisymmetric form can be considered as a representation of the Milky Way approximated by two Miyamoto disks with masses M_1 and M_2 respectively [Miyamoto and Nagai 1975]. The parameters we use in the present study are the same as in Katsanikas and Patsis [2011]. In our units, the distance R=1 corresponds to 1 kpc. For the Jacobi constant (hereafter called the "energy") E_j=1 corresponds to 43950 $(km/sec)^2$.

3. Spaces of section

A method to follow the stability of a family of periodic orbits in a system is by means of the "stability diagram" [Contopoulos and Barbanis 1985, Pfenniger 1985a]. The stability diagram gives the evolution of the stability of a family of periodic orbits in a system as one parameter varies, by means of the evolution of the stability indices b_1, b_2. In our case the parameter that varies is the energy E_j. Fig. 1 gives the evolution of the stability of the central family of periodic orbits x1 on the equatorial plane [Contopoulos and Papayannopoulos 1980], and its bifurcations for $-5.5 < E_j < -4.5$. We observe,

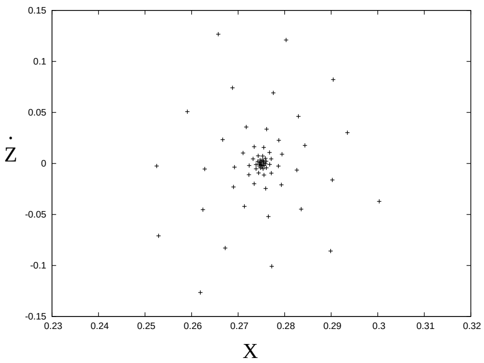

Fig. 2. 2D projection $(x, \dot{z})$ of the 4D surface of section at the neighborhood of a complex unstable (Δ) periodic orbit of the 3D family x1v1 for $E_j = -4.619$ (for 70 intersections).

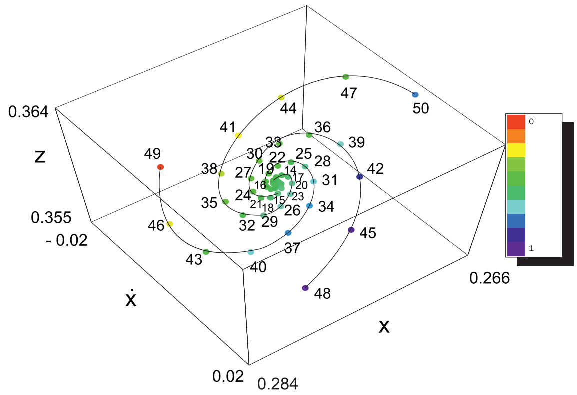

Fig. 3. The orbital behavior close to a complex unstable (Δ) periodic orbit of the 3D family x1v1 for $\Delta x = 10^{-4}$ and $E_j = -4.619$ (for 50 intersections). We use the $(x, \dot{x}, z)$ space for plotting the points and the $\dot{z}$ value to color them. Our point of view in spherical coordinates is given by $(\theta, \phi) = (32^o, 53^o)$.

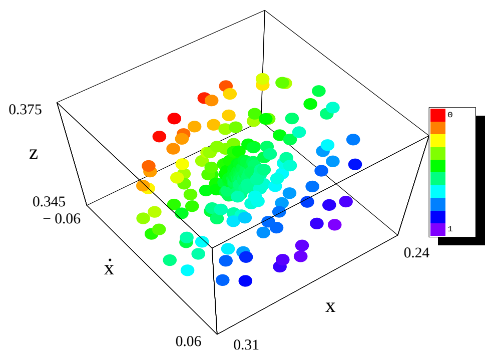

Fig. 4. The same case as Fig. 3 for 2000 intersections.

that x1 is initially stable and at E_j= -5.1644 it becomes simple unstable. There we have a $S \rightarrow U$ transition and a new 3D family, x1v1 [Skokos et al 2002a,b], is bifurcating and is stable. For E_j=-4.62 the family x1v1 becomes complex unstable and the stability indices meet each other. After that the values of $b_{1,2}$ are complex numbers.

We investigate the structure of the phase space by perturbing the initial conditions of a complex unstable periodic orbit in the 4D surface of section after a transition from stability to complex instability. For example we can apply a perturbation $\Delta x = 10^{-4}$ at the initial conditions of a complex unstable periodic orbit for E_j=-4.619 with initial conditions $(x_0, \dot{x}_0, z_0, \dot{z}_0) = (0.275137727, 0, 0.359838, 0)$. Then, the x initial condition will be $x_0 + \Delta x$. From previous papers [Contopoulos et al. 1994, Papadaki et al. 1995] we know that, for a number of intersections, a spiral appears in the consequents at the neighborhood of a complex unstable (Δ) periodic orbit in 2D projections of the 4D surfaces of section. This structure is encountered also in the case we study (Fig. 2). We observe that the consequents are confined and this means that we have a direct Hamiltonian Hopf bifurcation.

We apply the method of color and rotation to study the invariant surface in the neighborhood of the complex unstable periodic orbit. In Fig. 3 we present the orbital behavior close to the complex unstable periodic orbit for 50 intersections with the surface of section. We use the 3D $(x, \dot{x}, z)$ projection for plotting the points and the $\dot{z}$ values to color them. Our point of view is $(\theta, \phi) = (32^o, 53^o)$. We observe a spiral (with three spiral arms) in the neighborhood of the complex unstable periodic orbit. The first 13 points are very close to the center of the spiral and are not discernible in the figure. The 14th point is located on a spiral arm, the 15th point is located on another spiral arm and the 16th point is located on the third spiral arm. The 17th point is on the first spiral arm again and so on. In this way the points fill the space. Along every spiral arm we have a succession of colors (Fig. 3). In Fig. 3 we observe that if we begin from the center along the spiral arm going through the 15th point we have a succession of colors from green to light blue, light blue to blue and blue to violet. Along the spiral arm through the 16th point we observe a smooth color variation from green to light blue, to blue, to light blue, to green, to green-yellow, to orange-red. Finally along the third spiral arm we observe also a smooth color variation. Starting from the center of this spiral arm, we see that green becomes green-yellow, then yellow, green-yellow, green and finally light blue (Fig. 3).

Figure 4 depicts the same case as in Fig. 3 and we observe the orbital behavior close to the complex unstable periodic orbit for 2000 intersections with the surface of section. We cannot distinguish the spiral any more, but we observe a disk-like structure. The central area is saturated due to the presence of many points. This object has a very small thickness and is also slightly warped. Hereafter we will refer to this structure as the "disk" or "disk structure". In the terminology of Jorba & Ollé [2004] such structures are called confined tori. Small deviations from the pure planar geometry are due to a warp of the disk in the 3D space. On this disk structure, from left to right, we have a succession of colors from red to orange, orange to yellow, yellow to green, green to light blue, light blue to blue and blue to violet. For 10000 intersections we observe that the points fill the disk structure (Fig. 5), which has a smooth color variation. The smallest distance of the consequents on this disk structure from the complex unstable periodic orbit is 0.000042 and the largest distance is 0.059764 in the 3D projection $(x, \dot{x}, z)$ of the 4D surface of section. The consequents reach an outermost distance, then they move inwards reaching a minimum distance, then they move outwards etc. Some values for the minimum and maximum distances are given in Tables 1 and 2. We underline the fact, that the disk has an internal three-armed spiral structure. This means that if we choose arbitrarily a point on the disk, the subsequent consequents will follow a spiral pattern as the one presented in Figs. 3, 4 and 5, which lies on the disk. For this orbit we calculated also the "finite time" Lyapunov Characteristic Number (LCN), i.e.

$$LCN(t) = \frac{1}{t} \ln \left| \frac{\xi(t)}{\xi(t_0)} \right|,$$

where $\xi(t_0)$ and $\xi(t)$ are the distances between two points of two nearby orbits at times t = 0 and t respectively(see e.g. Skokos [2010]). We found, that initially it decreases and finally it levels off around 6×10^{-3} after about 4500 intersections (Fig. 6, lower blue curve).

We observe the same behavior (the same disk structure) if we apply a perturbation $\Delta x = 10^{-3}$ to the initial conditions of the complex unstable periodic orbit for E_j=−4.619 in the same way we did in the previous case for $\Delta x = 10^{-4}$. The only difference we find is that the minimum distance of the consequents from the complex unstable periodic orbit is now 0.000999 and the maximum distance is 0.054065. The minimum distance is 10 times larger than the minimum distance for a perturbation $\Delta x = 10^{-4}$ and for this reason we have a small hole at the center of the disk structure. Now if the

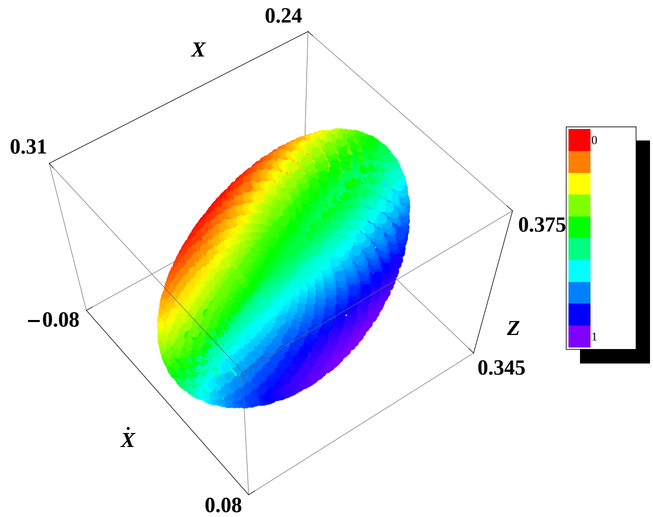

Fig. 5. The same case as Fig. 3 for 10000 intersections.

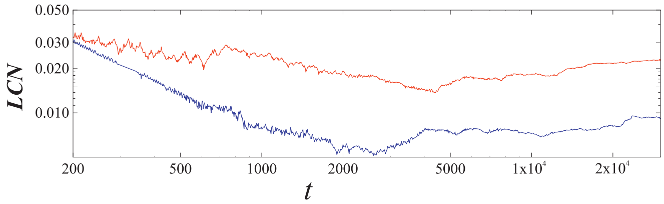

Fig. 6. The evolution of the two $LCN(t)$. The blue curve corresponds to the case of the confined torus, while the red to the case of the cloud.

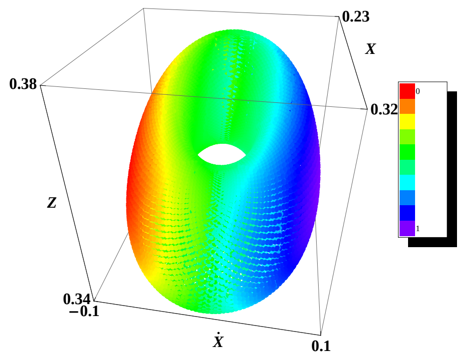

Fig. 7. The orbital behavior close to a complex unstable (Δ) periodic orbit of the 3D family x1v1 for $\Delta x = 10^{-2}$ and $E_j = -4.619$ (for 10000 intersections). Our point of view in spherical coordinates is given by $(\theta, \phi) = (15^o, 90^o)$.

Table 1. Some examples of points on the disk for a perturbation $\Delta x = 10^{-4}$ from the complex unstable periodic orbit for $E_j = -4.619$, which have maximum distance from the periodic orbit.

nth point	221	522	802	2679	8904
max distance	0.056284	0.058844	0.058453	0.059693	0.059764

Table 2. Some examples of points on the disk for a perturbation $\Delta x = 10^{-4}$ from the complex unstable periodic orbit for $E_j = -4.619$, which have minimum distance from the periodic orbit.

nth point	300	600	912	2780	8990
min distance	0.000338	0.000316	0.000042	0.000050	0.000173

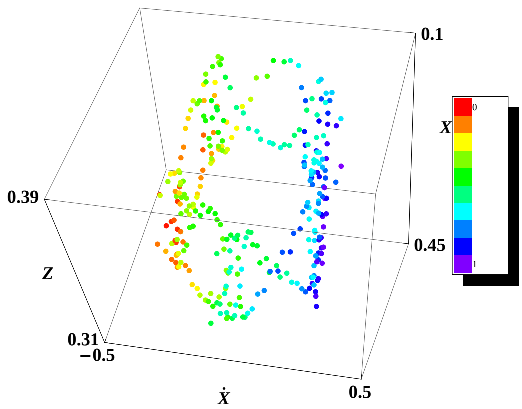

Fig. 8. The orbital behavior close to a complex unstable (Δ) periodic orbit of the 3D family x1v1 for $\Delta x = 10^{-1}$ and $E_j = -4.619$ (for 310 intersections). Our point of view in spherical coordinates is given by $(\theta, \phi) = (15^o, 90^o)$.

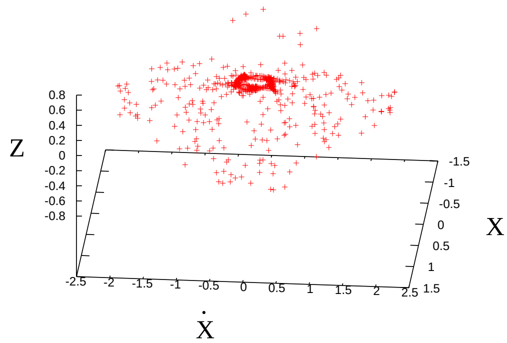

Fig. 9. The 3D projection $(x, \dot{x}, z)$ of the consequents close to a complex unstable (Δ) periodic orbit of the 3D family x1v1 for $\Delta x = 10^{-1}$ and $E_j = -4.619$ (for 3000 intersections). Our point of view in spherical coordinates is given by $(\theta, \phi) = (55^o, 95^o)$.

perturbation is even larger, $\Delta x = 10^{-2}$, we observe a different disk structure (Fig. 7). The new disk becomes thicker than the previous disk we have studied with initial $\Delta x = 10^{-3}$ or $\Delta x = 10^{-4}$ away from the periodic orbit. Now the "thickness" in the three coordinates is $(\Delta X, \Delta \dot{X}, \Delta Z) = (0.09, 0.2, 0.04)$ instead of $(\Delta X, \Delta \dot{X}, \Delta Z) = (0.07, 0.16, 0.03)$ we had before. On this "disk structure" we observe a smooth color variation from red to violet (Fig. 7). This means that the 4th dimension follows the topology of this structure in the 4D surface of section. The smallest distance of the consequents on this structure from the complex unstable periodic orbit is 0.009999 and the largest distance is 0.078655 in the 3D projection $(x, \dot{x}, z)$ of the 4D surface of section. Thus, the smallest distance of the consequents on the disk structure for the perturbation $\Delta x = 10^{-2}$ is now 100 times larger than the smallest distance of the $\Delta x = 10^{-4}$ perturbation. As expected the hole in middle of the "disk" is now even larger (Fig. 7).

Now we increase the perturbation by taking $\Delta x = 10^{-1}$, always for E_j=-4.619. The first approximately N=300 consequents form a toroidal surface. During this period the "finite time" $LCN(t)$ of the orbit decreases to a value 1.75×10^{-2} (Fig. 6, upper, red curve). Beyond that point it fluctuates as the time increases and finally increases and tends to level off around 2.5×10^{-2} after about 4700 intersections. On our 4D surface of section the consequents fill a cloud around the toroidal object during the same time.

In Fig. 8 we observe the first 310 consequents. Besides the points that form the toroidal object, we have included also the very first points that depart from it. These points correspond to the cuspy features we can observe in the red dense ring in Fig. 9. In Fig. 8 the 4th dimension $\dot{z}$ is represented by the

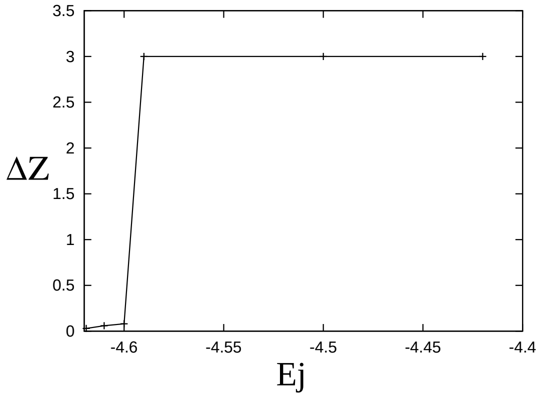

Fig. 10. Diagram of the ΔZ variation of the consequents close to a complex unstable periodic orbit versus E_j.

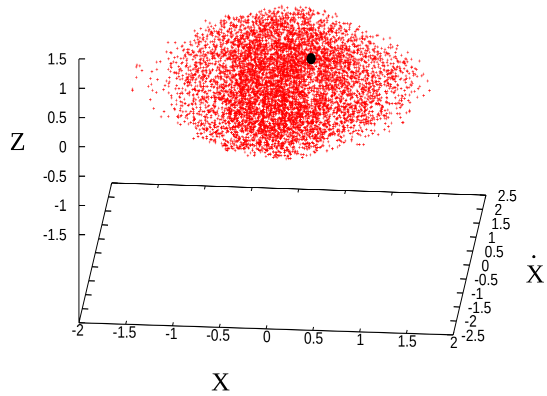

Fig. 11. The 3D projection $(x, \dot{x}, z)$ of the consequents close to a complex unstable (Δ) periodic orbit of the 3D family x1v1 for $\Delta x = 10^{-4}$ and $E_j = -4.50$ (for 4000 intersections). The periodic orbit is depicted by a black point. Our point of view in spherical coordinates is given by $(\theta, \phi) = (62^o, 5^o)$.

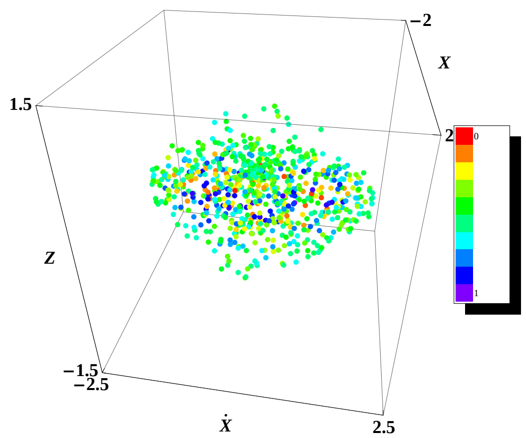

Fig. 12. The orbital behavior close to a complex unstable (Δ) periodic orbit of the 3D family x1v1 for $\Delta x = 10^{-4}$ and $E_j = -4.50$ (for 2000 intersections). Our point of view in spherical coordinates is given by $(\theta, \phi) = (55^o, 88^o)$.

colors. Smooth color variation in the consequents is again present and this means that we have a toroidal surface in the 4D space of section. By considering more points on the surface of section (Fig. 9), we observe that they deviate from this toroidal surface and they soon occupy a large volume of the phase space. This indicates stickiness [Contopoulos and Harsoula 2008].

As mentioned previously, the maximal LCN for the case of the cloud (Fig. 9) is around 2.5×10^{-2}, while the same index for the orbit of the confined torus (Fig. 5) is lower, 6×10^{-3}. This difference is expected by the nature of the two orbits. In the cloud we have scattered points in 4 dimensions, while in the case of the confined torus, chaos is due to the different maximum and minimum distances from the center reached as the orbit "fills" the disky structure of this torus (see Tables 1 and 2).

We choose now a $\Delta x = 10^{-4}$ deviation from the initial conditions of the periodic orbit, that gives a confined torus at $E_j = -4.619$ and we increase E_j. In Fig. 10 we depict the variation of the thickness ΔZ of the consequents in the 4D surface of section versus the energy E_j. We observe that for values of E_j between -4.62 and -4.59 we have small values of ΔZ and for values of E_j between -4.59 and -4.42 we have large values of ΔZ. The first interval of E_j corresponds to the disk structures that we described before. The second interval corresponds to the clouds of points that we find for values of the energy larger than -4.59. For example for $E_j = -4.50$ we observe a cloud of points with values of z from -1.5 to 1.5 (Fig. 11). The periodic orbit is depicted as a black point and it has initial conditions $(x_0, \dot{x}_0, z_0, \dot{z}_0) = (0.307260, 0, 0.432148, 0)$. In Fig. 12 we observe a mixing of colors for this cloud and this indicates a chaotic behavior in 4D space.

Let us investigate now the changes observed in the neighborhood of the complex unstable periodic orbit when we vary the energy. At the transition point of Fig. 10, for $E_j = -4.59$ and for a perturbation of the initial conditions equal to $\Delta x = 10^{-4}$, the first 800 consequents remain on a disk structure as we can see in Fig. 13. We note that the points do not suffice to fill densely the "disk". On this disk

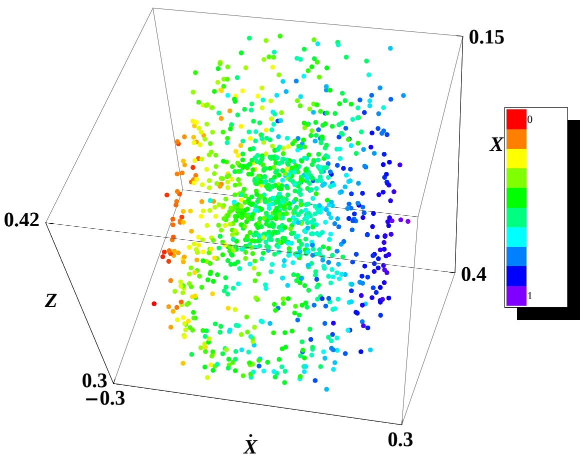

Fig. 13. The orbital behavior close to a complex unstable (Δ) periodic orbit of the 3D family x1v1 for $\Delta x = 10^{-4}$ and $E_j = -4.59$ (for 800 intersections). Our point of view in spherical coordinates is given by $(\theta, \phi) = (15^o, 90^o)$.

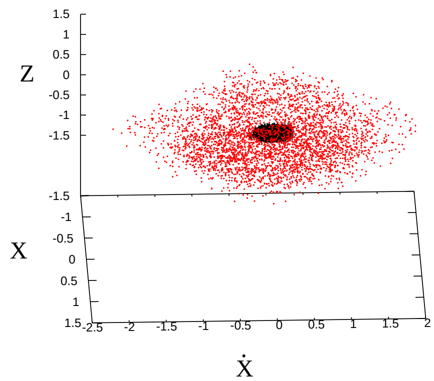

Fig. 14. The 3D projection $(x, \dot{x}, z)$ of the consequents close to a complex unstable (Δ) periodic orbit of the 3D family x1v1 for $\Delta x = 10^{-4}$ and $E_j = -4.59$ (for 4000 intersections). Our point of view in spherical coordinates is given by $(\theta, \phi) = (55^o, 88^o)$.

structure we observe a color succession from violet to blue, to light blue, to green, to yellow, to orange, to red. We underline that the succession of colors means that the 4th dimension $\dot{z}$ of the consequents lies on this disk structure. In Fig. 14 we see that if we integrate the orbit for more time, the consequents start to leave this disk structure (that is depicted with black color) and form a cloud of points around it. This is again a typical behavior of a sticky orbit.

4. Conclusions

In this paper we studied the phase space structure at the neighborhood of a complex unstable periodic orbit after a direct Hamiltonian Hopf bifurcation. Close to a Hamiltonian Hopf bifurcation we observe that:

(1) We have a spiral structure formed by the consequents at the neighborhood of complex unstable periodic orbits in the 2D projections of the 4D surface of section as in Contopoulos et al [1994] and Papadaki et al [1995]. Here we find that we have this spiral structure in the 3D projections and we observe a smooth color variation along their arms. This means that this spiral structure is a 4D object.

(2) The consequents near a complex unstable periodic orbit arrive at a maximum distance from the periodic orbit and they move inwards. By repeating this process, a disk structure is formed in the 3D projection of the 4D surface of section, which is called a confined torus [Pfenniger 1985a,b, Jorba & Ollé 2004 and Ollé et al 2004]. On this disk structure we observe a smooth color succession. This means that we have a disk structure (the confined torus) also in the 4D space of section.

(3) If we apply larger perturbations to the initial conditions we observe, that the disk structures become toroidals with smooth color variation and holes at their centers. For a critical value of the Δx perturbation of the initial conditions we observe for a number of intersections a toroidal surface with smooth color variation. However, later, the consequents leave this toroidal surface and move away occupying a larger volume in the phase space. This is a case of stickiness [Contopoulos & Harsoula 2008] in the case of complex instability and confined tori. This is the first time that we visualize stickiness in the neighborhood of a complex unstable periodic orbit.

(4) As the value of energy increases we do not find confined tori anymore, but clouds of points in the neighborhood of complex unstable periodic orbits. These clouds have mixing of colors. This means that we have strong chaos in the 4D space of section when we go far from the transition point from stability to complex instability.

(5) The calculation of the "finite time" LCN, gives a global value of the variation of the volume filled by the consequents of the orbits. We found

that the $LCN(t)$ curve levels off after more than 4500 intersections and is around 2.5×10^{-2} for the case of the cloud (Fig. 9), and around 6×10^{-3} for the confined torus (Fig. 5). On the other hand, the method of color and rotation gives in a much more direct and detailed way the volumes of the phase space occupied by an orbit during its integration. This is of particular importance in Galactic Dynamics.

Acknowledgments MK is grateful to the "Hellenic Center of Metals Research" for its support in the frame of the current research. This research has been partly supported by the Research Committee of the Academy of Athens under the project 200/739.

References

Bridges T.J., Cushman R.H. and Mackay R.S. [1995] "Dynamics near an irrational collision of eigenvalues for symplectic mappings" *Fields Inst. Comm.* **4**, 61-79.

Broer H.W., Hanssmann H. and Hoo J. [2007] "The quasi-periodic Hamiltonian Hopf Bifurcation" *Nonlinearity* **20**, 417-460.

Broucke R. [1969] "Periodic orbits in the elliptic restricted three-body problem" *NASA Tech. Rep.* 32-1360, 1-125.

Contopoulos G. and Papayannopoulos Th. [1980] "Orbits in weak and strong bars" *Astron. Astrophys.* **92**, 33-46.

Contopoulos G. and Barbanis B. [1985] "Resonant systems with three degrees of freedom" *Astron. Astrophys.* **153**, 44-54.

Contopoulos G. and Harsoula M. [2008] "Stickiness in Chaos" *Int. J. Bif. Chaos* **18**, 2929-2949.

Contopoulos G. and Magnenat P. [1985] "Simple three-dimensional periodic orbits in a galactic-type potential" *Celest. Mech.* **37**, 387-414.

Contopoulos G., Farantos S.C., Papadaki H. and Polymilis C. [1994] "Complex unstable periodic orbits and their manifestation in classical and quantum dynamics" *Phys. Rev. E* **50**, 4399-4403.

Contopoulos G. [2002] *Order and Chaos in Dynamical Astronomy* Springer-Verlag, New York Berlin Heidelberg.

Hadjidemetriou J.D. [1975] "The stability of periodic orbits in the three-body problem" *Celest. Mech.* **12**, 255-276.

Heggie D.C. [1985] "Bifurcation at complex instability" *Celest. Mech.* **35**, 357-382.

Jorba A. and Ollé M. [2004] "Invariant curves near Hamiltonian Hopf bifurcations of four-dimensional symplectic maps" *Nonlinearity* **17**, 691-710.

Katsanikas M. and Patsis P.A. [2011] "The structure of invariant tori in a 3D galactic potential" *Int. J. Bif. Chaos* (in press).

Miyamoto M. and Nagai R. [1975] "Three-dimensional models for the distribution of mass in galaxies" *Publ. Astron. Soc. Japan* **27**, 533-543.

Ollé M. and Pfenniger D. [1998] "Vertical orbital structure around the lagrangian points in barred galaxies. Link with the secular evolution of galaxies" *Astron. Astrophys.* **334**, 829-839.

Ollé M., Pacha J.R. and Villanueva J. [2004] "Motion close to the Hopf bifurcation of the vertical family of periodic orbits of L_4" *Celest. Mech. Dyn. Astr.* **90**, 89-109.

Ollé M., Pacha J.R. and Villanueva J. [2005a] "Quantitative estimates on the normal form around a non-semi-simple 1:-1 resonant periodic orbit" *Nonlinearity* **18**, 1141-1172.

Ollé M., Pacha J.R. and Villanueva J. [2005b] "Dynamics close to a non-semi-simple 1:-1 resonant periodic orbit" *Discrete Contin. Dyn. Syst. B* **5**, 799-816.

Ollé M., Pacha J.R. and Villanueva J. [2008] "Kolmogorov-Arnold-Moser aspects of the periodic Hamiltonian Hopf bifurcation" *Nonlinearity* **21**, 1759-1811.

Papadaki H., Contopoulos G. and Polymilis C. [1995] "Complex Instability" In: *From Newton to Chaos* ed by A.E. Roy, B.A. Steves, Plenum Press, New York, pg. 485-494.

Patsis P.A. and Zachilas L. [1994] "Using Color and rotation for visualizing four-dimensional Poincaré cross-sections:with applications to the orbital behavior of a three-dimensional Hamiltonian system" *Int. J. Bif. Chaos* **4**, 1399-1424.

Pfenniger D. [1985a] "Numerical study of complex instability:I Mappings" *Astron. Astrophys.* **150**, 97-111.

Pfenniger D. [1985b] "Numerical study of complex instability:II Barred galaxy bulges" *Astron. Astrophys.* **150**, 112-128.

Poincaré H. [1892] *Les Méthodes Nouvelles de la Mécanique Céleste* Gauthier Villars, Paris I (1892), II (1893), III (1899); Dover (1957).

Skokos Ch. [2001] "On the stability of periodic orbits of high dimensional autonomous Hamiltonian systems" *Physica D* **159**, 155-179.

Skokos Ch. [2010] "The Lyapunov Characteristic Exponents and their Computation", *Lect. Not. Phys.* **790**, 63-135

Skokos Ch., Patsis P.A. and Athanassoula E. [2002a] "Orbital dynamics of three-dimensional bars-I. The backbone of three-dimensional bars. A fiducial case" *Mon. Not. R. Astr. Soc.* **333**, 847-860.

Skokos Ch., Patsis P.A. and Athanassoula E. [2002b] "Orbital dynamics of three-dimensional bars-II. Investigation of the parameter space" *Mon. Not. R. Astr. Soc.* **333**, 861-870.

Van der Meer J-C. [1985] *The Hamiltonian Hopf Bifurcation* Lecture Notes in Mathematics Vol. 1160, Berlin.

Wolfram S. [1999] *The Mathematica book* Wolfram media & Cambridge Univ. Press.